Magneto-optics of acceptor-doped GaAs/$Ga_{1-x}Al_xAs$ heterostructures in the quantum Hall regime: Resonant magnetoexcitons and many-electron effects

Pawel Hawrylak
Max-Planck-Institut für Festkörperforschung, 7000 Stuttgart 80, Germany
and Institute for Microstructural Sciences, National Research Council of Canada, Ottawa, Canada K1A OR6

Nicolas Pulsford and Klaus Ploog
Max-Planck-Institut für Festkörperforschung, 7000 Stuttgart 80, Germany
(Received 13 April 1992; revised manuscript received 27 July 1992)

The effect of carrier density, magnetic field, and final-state interactions on the radiative recombination of electrons with holes localized on acceptors in GaAs/$Ga_{1-x}Al_xAs$ heterostructure is investigated. In the high-density regime, strong oscillations of the position and intensity of the emission spectrum as a function of the magnetic field are observed at even filling factors. In the low-density regime, an almost perfect cancellation of many-body effects in emission from the first subband is observed accompanied by oscillations of the emission intensity of the second subband magnetoexcitons. The peaks in the intensity of the second subband emission occur at the integer values of the ratio of the subband separation to the cyclotron energy. These results are explained by the calculated self-consistent subband structure and emission spectrum including shake-up and excitonic effects.

I. INTRODUCTION

The photoluminescence spectra of ultraclean modulation-doped quantum wells and heterojunctions are determined by the recombination of the two-dimensional electrons with photoexcited holes. For "free" holes, the main contribution to the emission spectrum comes from transitions involving low-energy electron states (small k vector) while very little information is available about the electronic states in the vicinity of the Fermi surface, thereby making the correlation of optical data with transport measurements difficult. This problem can be circumvented by localizing the holes either on alloy disorder fluctuations[1,2] or on intentionally introduced acceptors[2,3] or by coupling with higher subbands.[4,5] The latter approach was used by Chen *et al.*[4] with specially designed modulation-doped asymmetric quantum wells to show the enhancement of the tail of the emission spectrum in the vicinity of the Fermi level. This enhancement at the Fermi edge[6] [Fermi-edge singularity (FES)] was only present when the Fermi level in the populated ($n=1$) subband approached the empty subband ($n=2$). Both the FES ($n=1$) and the emission by photoexcited carriers in the empty subband ($n=2$ magnetoexcitons) were found to be sensitive functions of the magnetic field and correlated with the filling factor and resistivity in the quantum Hall regime. Subsequently, several groups[7,8] have used the magnetoexciton as a spectroscopic probe of the integer and fractional quantum Hall effect (IQHE and FQHE, respectively).

The calculation of the emission spectrum of modulation-doped quantum wells in the IQHE regime has been carried out by Uenoyama and Sham[9] using the self-consistent Born approximation for disordered electronic states and a rigid Fermi sea (Mahan exciton) approximation for excitonic corrections. In the same spirit the theoretical explanation for the enhancement of the FES in the presence of the $n=2$ subband has been proposed by Mueller.[10] A different explanation has been proposed by one of us.[11,12] In Ref. 10 the enhancement takes place when the Mahan exciton associated with the rigid Fermi surface of the occupied subband resonates with the exciton state originating from the empty subband. Clearly, such a mechanism is plausible only for an attractive electron-hole interaction and it completely neglects the dynamical response of the Fermi sea. It is known for a localized hole that the Fermi sea mediated scattering processes remove Mahan excitons completely.[11] An exact calculation for the emission spectrum with a localized hole[11,12] which includes both the dynamical response of the Fermi sea and excitonic (final-state) effects reveals that the enhancement is due to the mixing of the subband states by the photoexcited hole and due to virtual excitations of electron-hole pairs involving the higher subband. These processes are enhanced by the proximity of the Fermi level and the higher subband, whose energy separation from the Fermi level can be varied by sweeping the magnetic field.[4,12] Theoretically, the calculated intensity oscillation[12] correlates with the subband separation and, by coincidence, with even filling factors. Experimentally,[4] on the other hand, the observed oscillations in emission from magnetoexcitons in the empty subband correlated with odd filling factors. However, for free valence holes excitonic effects make the correlation of the position of oscillations with the filling factor difficult.

To understand the correlation of emission oscillations with magnetic field and their relation to the many-electron effects in the dynamical response of the Fermi sea, we have carried out experiments and calculations of the emission spectra in acceptor δ-doped heterostructures as a function of magnetic field and carrier density. We concentrate on a recognized spectral feature below the

 ©1992 The American Physical Society

band-to-band recombination originating from the acceptor-bound exciton,[3] the B line. Due to the presence of free carriers, only the photoexcited valence hole remains bound to the negatively charged acceptor. The localization of holes means that the optical transitions in the vicinity of the Fermi level have significant spectral weight and are hence ideal for the study of the Fermi-edge singularity. The calculations of Refs. 12 and 13 are extended to include magnetic field, disorder, and empty subbands. We separate the emission by photoexcited carriers (magnetoexcitons) from the FES (due to equilibrium carriers) and demonstrate that the recombination of photoexcited carriers in empty subbands measures the dynamical response of the Fermi sea to the annihilation of the valence hole.

The remaining part of this paper is organized as follows: Sec. II contains a theoretical discussion of the recombination process; Sec. III A presents experiments and calculations of high-carrier-density samples with the Fermi level in the vicinity of the second subband; Sec. III B studies magnetoexcitons associated with empty subbands in the presence of the Fermi sea; Sec. IV summarizes our results.

II. THEORY OF EMISSION

A. Two-subband Fermi-edge singularity

We study a single modulation-doped $GaAs/Ga_xAl_{1-x}As$ heterostructure with electron density n_s, in the range of 10^{11} cm^{-2} with typically one or two subbands occupied. The heterostructure[3] contains a δ-doped layer of acceptors (Be) with a sheet density of 2×10^{10} cm^{-2} at the distance $z_a=250$ Å away from the $GaAs/Ga_xAl_{1-x}As$ interface. In a magnetic field perpendicular to the interface electrons occupy ladders of disorder broadened Landau levels "l" associated with different subband "n".

The physical picture of the recombination process is very simple: prior to illumination (and after the recombination) our system consists of N electrons and a single negatively charge acceptor which acts as a repulsive scattering center for electrons. The single-particle states and energies for N conduction electrons in a heterostructure and one electron trapped on the acceptor are denoted by $|\lambda\rangle$ and e_λ and $|h\rangle$ and $-\omega_a$, respectively. This is our final basis. It contains all the single-particle effects of the confining potentials (subband structure), disorder, and magnetic field. The effect of electron-electron interactions are included via static self-energies. Upon illumination, one electron is added to the conduction band and a hole from the valence band is localized by the negatively charged acceptor, making it a neutral weak scattering center. The single-particle states and energies of $(N+1)$ conduction electrons in a heterostructure in the presence of a neutral acceptor are denoted by $|k\rangle$ and e_k.

The emission spectrum $E(\omega)$ involves the emission of a photon with frequency ω with one of the $N+1$ conduction electrons making a transition to the empty level (hole) localized on the acceptor. The annihilation of the hole changes the potential seen by all electrons in the conduction subband from that of a charge neutral to a negatively charged acceptor and this makes the transition a many-electron effect. The emission spectrum $E(\omega)$ is written in terms of a time-dependent emission function $E(t)$:[11–13]

$$E(\omega)=2\,\mathrm{Re}\int_0^\infty dt\, e^{-i(\omega-\omega_{\max})t}E(t)\ . \tag{1}$$

The maximum photon frequency $\omega_{\max}$ is given by the difference between the ground-state energies of $N+1$ particles before and after emission: $\omega_{\max}=E_i(N+1)-[E_f^0(N)+(-\omega)]$. $E_f^0(N)$ is the ground-state energy of the normal (final) state, i.e., without the photoexcited electron. The time-dependent emission spectrum $E(t)$ of course assures that no frequencies larger than the maximum allowed frequency $\omega_{\max}$ contribute to the frequency spectrum. The key role in the calculation of the emission spectrum is played by matrix elements[13,14] $\Phi(t)_{k,k'}=\langle k|\exp(-itH_f)|k'\rangle$. $\Phi(t)_{k,k'}$ describes the propagation of the initial single-particle states $|k\rangle$ by the final-state Hamiltonian H_f and is determined by the final-state energies and the overlap matrix elements $\langle k|\lambda\rangle$ between initial and final states:[13,15]

$$\Phi(t)_{k,k'}=\sum_\lambda \langle k|\lambda\rangle e^{-ie_\lambda t}\langle\lambda|k'\rangle\ . \tag{2}$$

The overlap matrix elements satisfy the usual Wannier equation:

$$e_k\langle k|\lambda\rangle+\sum_{k'}V_{k,k'}\langle k'|\lambda\rangle=e_\lambda\langle k|\lambda\rangle\ . \tag{3}$$

The matrix elements are written in the initial basis. The interaction $V_{k,k'}$ is the change in one electron potential between initial and final bases and corresponds to a repulsive scattering potential due to the screened charge of the hole localized on acceptor. The scattering potential of the neutral acceptor is assumed to be negligible.

The emission spectrum $E(t)$ is now written in terms of the matrix $\Phi_{k,k'}$ built out of all initially occupied electronic states, i.e., $k,k'<k_F$, where k_F is the highest occupied state, including the photoexcited electron:

$$E(t)=e^{iE_f^0t}\det(\Phi(t))\sum_{k,k'\le k_F}m_k\Phi^{-1}_{k,k'}(t)m_{k'} \tag{4}$$

The first term in Eq. (4) [$\det(\Phi)$] describes the shake-up of the Fermi sea due to the disappearance of the valence hole, while the last term describes vertex corrections, i.e., the scattering of the hole (Φ^{-1}) inside the Fermi surface by a repulsive potential in the final-state Hamiltonian H_f. This scattering process is mediated by exchange of the photocreated hole with holes (empty states) above the Fermi surface. The Fermi sea hole optical matrix elements $m_k=p_{vc}\langle h|k\rangle$ correspond to a transition from a conduction state $|k\rangle$ to a localized state $|h\rangle$. p_{vc} are the conduction- to valence-band momentum matrix elements and $\langle h|k\rangle$ is the overlap of the conduction and localized electron envelope wave function.

Equation (4) involves the states of the photoexcited system while one wants to measure the states of the system in equilibrium. This is done by transforming Eq. (4) into

the final basis. We define matrix $G_{\lambda,\lambda'}$ which describes the propagation of the hole in the Fermi sea in the final-state basis as $G_{\lambda,\lambda'}(t)=\sum_{k,k'\le k_F}\langle\lambda|k\rangle\Phi^{-1}_{k,k'}(t)\langle k'|\lambda'\rangle$. Using the relationship between the initial matrix elements m_k and final basis matrix elements m_λ given by $m_k=\sum_\lambda m_\lambda\langle\lambda|k\rangle$, and the identity $\det(\varphi)=\exp(\mathrm{Tr}\{\ln(\phi)\})=\exp(-iC(t))$, one can show that the vertex (G) and self-energy (C) functions satisfy a set of *nonlinear* differential equations:

$$\frac{\partial}{\partial t}G_{\lambda,\lambda'}(t)=-ie_\lambda G_{\lambda,\lambda'}(t)+i\sum_{\lambda''}G_{\lambda,\lambda''}(t)e_{\lambda''}G_{\lambda'',\lambda'}(t)\ ,$$
$$\frac{\partial}{\partial t}C(t)=2\sum_\lambda e_\lambda G_{\lambda,\lambda}(t)\ . \tag{5}$$

The final expression for the emission[11–13] function $E(t)$ is now given simply in terms of the vertex G and self-energy corrections C:

$$E(t)=e^{iE_f^0 t}e^{-iC(t)}\sum_{\lambda,\lambda'}m_\lambda e^{+ie_\lambda t}G_{\lambda,\lambda'}(t)m_{\lambda'}\ . \tag{6}$$

An important consequence of working in the final-state basis is that *all* the single-particle states of the final basis (e.g., all subband states mixed by the final-state potential) contribute to the frequency spectrum of the emission $E(t)$, irrespective of whether they are occupied or empty in the final ground state of the system. The filling of phase space of initial states enters via the initial condition for the matrix $G(0)$:

$$G_{\lambda,\lambda'}(0)=\sum_{k\le k_F}\langle\lambda|k\rangle\langle k|\lambda'\rangle\ .$$

The effect of an empty subband on the emission spectrum is twofold: the subband mixing due to the hole potential affects the overlap matrix elements (and initial conditions) and the electron-hole pair excitation. The closer the Fermi level to the bottom of the empty subband, the larger the mixing. In addition to this static excitonic correction, a dynamical response (shake-up) of the Fermi surface in terms of intersubband electron-hole pair excitations leads to an enhancement of the emission at the Fermi level. We wish to emphasize again that the FES always corresponds to a repulsive final-state interaction, i.e., switching off the valence hole potential. The initial state, on the other hand, is determined by the charge of the impurity-valence hole complex.

B. Subband magnetoexcitons

We now turn our attention to the effect of photoexcited carriers in an otherwise empty subband on the emission spectrum. To study this separately from the response of equilibrium carriers, the Fermi level must be sufficiently separated from the bottom of the empty subband. We consider N carriers in the lowest subband occupying initial single-particle states $k<k_F$ and one photoexcited carrier in a higher subband in some initial state $|K\rangle$. These single-particle states might include the presence of the photohole via the Wannier equation. It is understood that $e_K\gg e_F$ so that we can neglect any exchange processes between the equilibrium and the photoexcited carriers, i.e., matrix elements $\Phi(t)_{k,K}$. The emission spectrum now separates into two contributions: one from equilibrium carriers and one from photoexcited carriers. The photoexcited carrier contribution can be written as

$$E(t)=\exp\{itE_i(N)-iC(t)\}m_K^2e^{i(e_K+\omega_a)t}\ . \tag{7}$$

It is a convolution of a single-particle transition superimposed with the shake-up process of the electron gas due to the annihilation of the valence hole. It is easily identified as the Green's function of the valence hole in the presence of the electron gas.[16] This is to be contrasted with the main subband emission which is a convolution of excitonic effects (due to the creation of the hole in the Fermi sea) and shake-up processes. To emphasize the role of the second-subband emission as a probe of the electron gas we can rewrite the emission spectrum in terms of exact initial $|i\rangle$ and final $|f\rangle$ eigenstates of the N electron Hamiltonian:

$$E_2(t)=m_K^2e^{iE_Kt}\exp(it\delta E_g)\times\sum_f|\langle i|f\rangle|^2\exp[it(E_f^0-E_f)]\ . \tag{8}$$

The overall shift of the emission line δE_g is governed by the change in the ground-state energy of the N electron system due to annihilation of the valence hole. The single-particle transition is broadened by the excitation spectrum of the electron gas. Any gap in the excitation spectrum, either cyclotron, Zeeman, or in the FQHE regime leads to the narrowing of the emission line and a development of a shoulder. It should be stressed that the rigid Fermi sea picture, or Mahan exciton approximation, completely neglects these shake-up effects. The effect of the Fermi sea is only via screening of the valence hole potential.

In contrast to the complicated line shape, the total intensity I_0, however, is completely unaffected by the presence of free carriers and is given by the initial-state single-particle (excitonic or free-electron–bound-hole pair) oscillator strength $I_0=m_K^2$. Hence for acceptor samples the oscillator strength I_0 should not be affected by the crossing of Landau levels of the first and second subband. In contrast, for free holes the initial state is a magnetoexciton and the oscillator strength should change dramatically by the subband Landau-level mixing.

III. EXPERIMENTAL MEASUREMENT

A. Emission in the high-density regime ($E_F\sim E_2$)

Photoluminescence measurements are performed in magnetic fields up to 13 T at a temperature $T=1.5$ K. The heterostructure is excited with an Ar^+ laser and the luminescence is dispersed through a 1-m double spectrometer and detected by a cooled GaAs photomultiplier tube. The carrier concentration in the heterostructure is tuned by varying the incident laser power.[3] Typical laser intensities are in the range 10^{-5}–10^{-2} W cm^{-2} giving electron densities in the range 1.9–4.3×10^{11} cm^{-2}. In each case, we measure the emission spectra correspond-

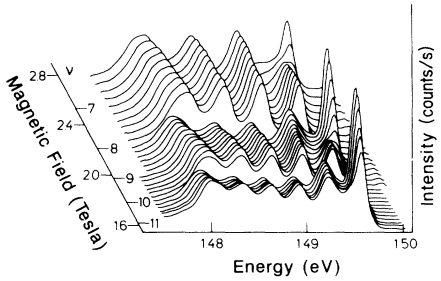

FIG. 1. The measured luminescence spectra for magnetic fields in the range 1.64–2.79 T corresponding to filling factors $\nu=10.8-6.3$ for a high carrier density $n_s=4.3\times10^{11}$ cm^{-2}. The intensity of the highest Landau level is strongly enhanced towards even filling factor when the Fermi level approaches the second subband.

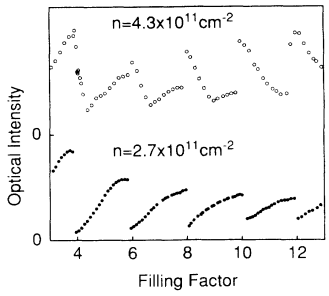

FIG. 3. The luminescence intensity at the Fermi energy for a high carrier density (upper curve, $n_s=4.3\times10^{11}$ cm^{-2}) and a low carrier density (lower curve, $n_s=2.7\times10^{11}$ cm^{-2}). In the low-carrier-density case, the second subband plays no role and no enhancement of the optical intensity towards even filling factors is observed.

ing to the recombination of electrons with holes bound to acceptors (B lines).

We first study the high-carrier-density limit $n_s=4.3\times10^{11}$ cm^{-2}, where the Fermi energy lies in the vicinity of the second subband. The experimentally estimated Fermi level (E_F) and subband separation (Δ) are $E_F=15.0$ meV and $\Delta=14.3$ meV. Luminescence emission spectra are shown in Fig. 1 for the magnetic field B increasing from 1.64 T ($\nu=10.8$) to 2.79 T ($\nu=6.3$). The data are viewed from an angle to resolve the spectral features more clearly. Transitions involving all occupied electron Landau levels are observed. The most striking feature is the intensity of the highest occupied Landau level (at the Fermi energy). This shows a dramatic increase as an even filling factor is approached followed by an abrupt fall over $\sim1\%$ magnetic-field change as the filling factor is passed. The fall is accompanied by a discontinuous energy shift and increase in intensity of the remaining occupied Landau levels. The measured luminescence energies of the Landau levels are plotted as a function of magnetic field in Fig. 2. The energy discontinuity is the same for each Landau level in the first subband, and the Landau-level separation remains equal to the cyclotron energy at all magnetic fields. Only the separation between the first and second subbands changes and hence we ascribe these oscillations in line position as the response of the confining potential to changes in the electron distribution by the magnetic field.[5,17] In Fig. 3, we plot the luminescence intensity at the Fermi energy as a function of filling factor ν (upper curve) and compare its behavior with data for a lower carrier concentration (lower curve) where the second subband plays no role. For an almost full upper Landau level, there is a smooth decrease in intensity as it starts to depopulate. However, when the Fermi energy approaches the unoccupied second subband, the optical intensity is strongly enhanced and peaks at the even filling factor, even though the level is now virtually empty of carriers. In contrast, in the lower curve where the second subband plays no role, there is a gradual decrease in intensity as the level empties and no enhancement at the Fermi edge.

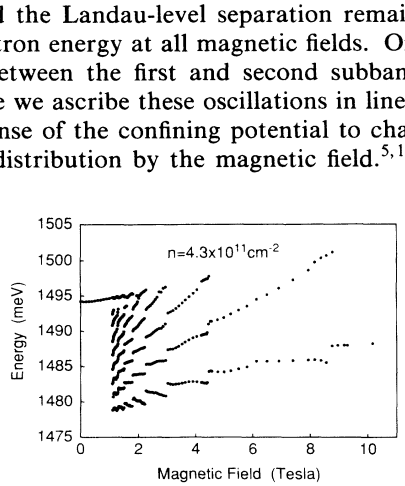

FIG. 2. The measured transition energies of the Landau levels as a function of magnetic field for a high carrier density $n_s=4.3\times10^{11}$ cm^{-2}. The discontinuities in level energy occur at even filling factors.

To understand these effects, we perform a self-consistent calculation of subband levels in a magnetic field and for finite temperature.[18,19] The effect of disorder is taken into account rather crudely by assuming a Gaussian density of states $D(E)$:

$$D(E)=\sum_n \frac{1}{\sqrt{2\pi}\Gamma\pi l_0^2}\sum_{l=0}^{\infty}\exp\{-(E-E_{n,l})/2\Gamma^2\}\ . \quad (9)$$

Here, $E_{n,l}=E_n+l\hbar\omega_c$ are subband Landau-level energies, Γ is the broadening of Landau levels, $\hbar\omega_c$ is cyclotron energy, and l_0 is the magnetic length. The choice of $\Gamma=0.3(B)^{1/2}$ meV is in line with previous work.[9] Other parameters include the electron density $n_s=4.3\times10^{11}$ cm^{-2}, the depletion charge $N_D=4.6\times10^{11}$ cm^{-2}, the acceptor sheet density $N_A=2.0\times10^{10}$ cm^{-2}, and the acceptor position $z_a=250$ Å. The actual transition energies involve energies of electrons $E_{n,l}$ and the hole energy ω_a. The hole is localized on the acceptor, and so the hole energy changes according to the changes of the self-consistent Hartree potential $V_H(z=z_a)$ at the position of the acceptor. Approximately, the energy of emitted photons is equal to $\omega_{n,l}=\omega_a+E_{n,l}-V_H(z_a)$, where ω_a is the bare transition energy. Hence the transition energies probe both the energy levels of the electrons and the spatial distribution of the Hartree potential.

In Fig. 4, the self-consistently calculated transition energies, the chemical potential μ, and the electron density n_s in the second subband are plotted as a function of magnetic field. The oscillations in line positions are

identified with the transfer of carriers due to partially occupied first-subband Landau levels crossing the lowest Landau level of the second subband. The finite width of the Landau levels means that close to the crossing point, a very small population ($n_s \sim 10^{10}$ cm^{-2}) of carriers is present in the second subband. Due to the large spatial extent of the second-subband wave function, even a very small carrier density leads to change in the self-consistent Hartree potential V_H.[5,17] We find that the changes in the Hartree potential at the position of the acceptor combined with the electron confinement are responsible for the decrease of transition energies with increasing magnetic field and hence allow us to spectroscopically probe the spatial distribution of the Hartree potential.

The calculations of Hartree energy levels, however, do not include effects of final-state interactions on the transition energies and emission line shape. To understand the oscillations of intensity as a function of magnetic field, especially the increase in intensity with decreasing population of the highest occupied Landau level, we have carried out an exact calculation of the emission spectrum for a model short-range electron-hole potential. Details of a similar calculation in a magnetic field have been given in Ref. 12 while the acceptor-related emission has been discussed in Ref. 13. We consider the initial single-particle basis as for a charge neutral acceptor while the final basis contains the negatively charged acceptor. Only zero angular momentum electron states contribute to the emission spectrum. Without disorder, there is only one zero angular momentum state per Landau level. However, the different angular momentum channels are mixed by the disorder and this we model by using a Gaussian density of states. The effect of localization is neglected. We solve the Wannier equation for Gaussian-broadened Landau levels with the density of states given by Eq. (7) and a short-ranged potential for the acceptor[12,13] $V(k,k') = V_0 m_{n,l} m_{n'l'}$. The initial matrix elements are given by $m_{n,l} = m_n\{-l\hbar\omega_c/E_b\}$, where E_b is the binding energy of the hole. The ratio of optical matrix elements from our self-consistent calculations is $m_2/m_1 = 3$, and we take $V_0 = 1.0$. The broadening of Landau levels due to disorder turns out to be important. When the Fermi level lies in the center of the Landau level, intra-Landau-level electron-hole pair excitations lead to a Fermi-edge singularity in the emission spectrum. This is illustrated in Fig. 5(a), where the exact emission spectrum (solid line) corresponding to a filling factor $\nu = 4.84$ is compared with the emission spectrum without final-state interactions (broken line). For this filling factor the second-subband Landau level is well separated from the partially populated highest first-subband Landau level. The effect of repulsive final-state potential is to shift and redistribute the oscillator strength of emission lines corresponding to filled Landau levels to higher energies, and increase the emission intensity at the Fermi level (FES). As the magnetic field is increased and the Landau level depopulates further, the character of response changes from a collective (dominated by the dynamical response of many electrons) to a single particle, excitonlike. We illustrate this in Fig. 5(b), where the calculated emission spectrum for $\nu = 4.18$ is shown. For this filling factor, both first and second subbands are weakly populated by carriers. Without the presence of the second subband, the emission from the vicinity of the Fermi level would have been small due to depopulation. The emission including the second subband but without final-state interactions is strong due to the large matrix elements (broken line). The effect of the repulsive final-state acceptor potential (solid line), however, is to reduce the intensity at the Fermi level when compared with the noninteracting emission. The decrease of intensity can be simply understood. Since the valence hole is localized on the acceptor, the repulsive finite-state acceptor potential reduces the overlap of the electron and hole wave function. Hence, in the experiment, the increase in emission towards even filling factors is due to population of the second subband with a higher optical matrix element. The calculation shows that the strength of the emission is reduced by the final-state interactions. This helps to explain the fact that the enhancement observed here of emission at the Fermi level is much smaller than that observed in Ref. 4. For a detailed comparison with experiment, the effect of electron-electron interactions, screening, and localization on the emission spectrum should be included. We relegate this nontrivial task to a future publication.

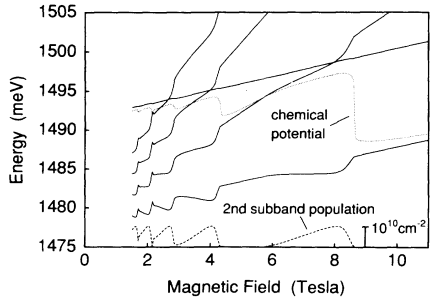

FIG. 4. Calculated transition energies (——), chemical potential (· · · ·), and occupation of the second subband (— — —) as a function of magnetic field for the high carrier density ($n_s = 4.3\times10^{11}$ cm^{-2}). The curve of the second subband occupancy has been offset; in the high field limit, the second subband is unoccupied.

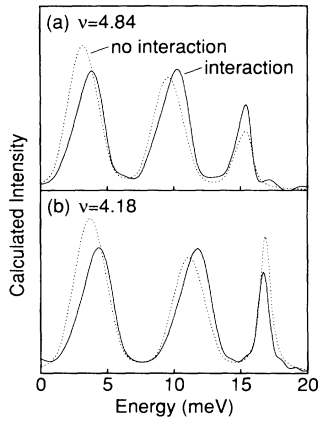

FIG. 5. Calculated emission spectra for different filling factors with (——) and without (— — —) electron-hole interaction for filling factor $\nu = 4.84$ (second subband empty) and filling factor $\nu = 4.18$ (second subband partially occupied).

B. Second-subband emission ($E_F \ll E_2$)

We now turn our attention to the use of the second-subband emission as a spectroscopic probe of the degenerate electron gas. By increasing illumination we reduce the carrier density[3] and increase the separation of the second-subband energy and the Fermi energy. The lowest carrier density studied is $n_s = 2\times10^{11}$ cm^{-2}, with measured Fermi energy $E_F = 6.2$ meV and subband separation $\Delta = 9.5$ meV. The luminescence spectra are now dominated by emission from the occupied Landau levels in the first subband with only a weak feature corresponding to the emission from the second subband. The transition energies of the subband Landau levels are plotted in Fig. 6 as a function of magnetic field. We observe almost no oscillations of the first-subband Landau-level transition energies with magnetic field (or filling factor ν). This contrasts with large oscillations reported for the recombination of electrons with free holes in doped quantum wells, which is attributed to the oscillation of the valence hole self-energy with magnetic field.[1,9]

The valence hole self-energy is due to the interaction with conduction electrons. The mobile hole drags with itself an electron cloud and lowers its energy. In the case of a free hole, the dynamic response (screening) of the electrons varies with magnetic field and leads to the oscillation in the valence hole self-energy. In comparison, a negatively charged acceptor reduces the electron density in its neighborhood. Hence, when the hole is trapped by an acceptor, the hole and acceptor electronic clouds cancel each other. This is just another way of saying that the acceptor is charge neutral. Thus the only changes observable in acceptor samples are changes in electron self-energy. As predicted by theory,[9] the experiment shows that these changes are very small.

Let us now turn our attention to the second-subband emission. The position of the emission line appears to be completely unaffected by the changes in the electron gas and follows the center of the second-subband lowest Landau level. This behavior is unexpected. The valence hole potential mixes the Landau levels in both subbands and one would expect that the emission line shows an anticrossing behavior whenever a first-subband Landau level crosses the lowest Landau level of the second subband. However, as is evident from Eq. (7), the second-subband recombination involves only the initial state, i.e., the electron state in the presence of a neutral acceptor. No mixing should be observed, in agreement with experiment.

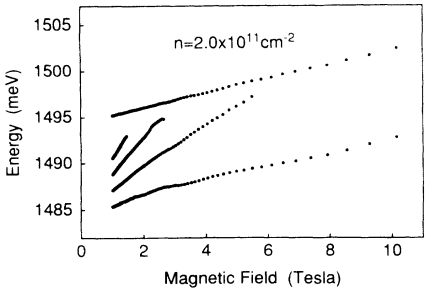

FIG. 6. The measured transition energies of the Landau levels as a function of magnetic field for a low carrier density ($n_s = 2.0\times10^{11}$ cm^{-2}).

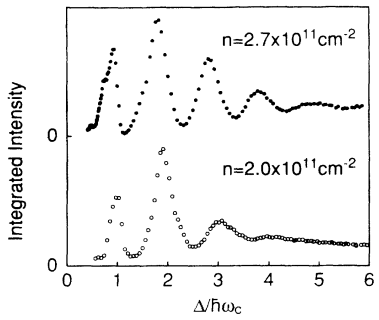

FIG. 7. The integrated intensity of the second subband as a function of $\Delta/\hbar\omega_c$ for two different low carrier densities. The subband separations are $\Delta = 10.7$ meV ($n_s = 2.7\times10^{11}$ cm^{-2}) and $\Delta = 9.5$ meV ($n_s = 2.0\times10^{11}$ cm^{-2}). No correlation with filling factor ($\nu \alpha 1/\hbar\omega_c$) is observed in these cases.

In contrast, an emission involving holes localized by potential fluctuations should reveal an anticrossing behavior, inversely periodic in Δ/B.[12]

The second-subband emission line follows the center of the Landau level, even though it is sparsely populated. Hence we conclude that states in the tail of the Landau level do not contribute to radiative recombination and only the extended states from the center of the Landau level contribute to the emission. The total integrated intensity I_2 is proportional to the oscillator strength of the second-subband transition m_K^2 times the population of the extended states ν_2: $I_2 = m_K^2 \nu_2$. Shake-up effects do not contribute to the integrated intensity and changes in screening by the equilibrium carriers as a function of the magnetic field should not affect extended states of the second-subband Landau level in a significant way. Experimentally, we observe strong oscillations in the integrated intensity of the second-subband emission. Contrary to the case of free holes,[4] these do not correlate with filling factor ν. However, as demonstrated in Fig. 7, the oscillation period does correlate with $\Delta/\hbar\omega_c$.[20] We believe that this is a population effect: whenever the first-subband Landau level crosses the second subband, the photoexcited electrons in the first-subband Landau level transfer to the photoexcited population of the second subband, leading to the increase of emission intensity at integer multiples of $\Delta/\hbar\omega_c$. Note that the carrier transfer to lower Landau levels in the first subband is slow because only the uppermost level is partially occupied. We are therefore in a position to measure the carrier population directly, and hence relaxation rates in the quantum Hall regime.

IV. SUMMARY

We have studied the photoluminescence from electrons in a GaAs/$Ga_xAl_{1-x}As$ heterostructure with holes bound to a δ-doped layer of Be acceptors. Our theoretical analysis focuses on the interplay between the Fermi level and the second subband in the recombination process and separates the emission by photoexcited carriers

from the Fermi-edge singularity. We compare the theoretical model to experiment by tuning the electron concentration in a heterostructure to separate the second subband from the Fermi level and this provides a unique opportunity to study the dynamical response of the Fermi sea.

In the high-carrier-density regime, where the Fermi level lies close to the second subband, we observe strong oscillations in optical intensity at the Fermi level coupled with discontinuous shifts in the transition energies of the occupied Landau levels which correlate with even filling factors. The energy shifts are due to change in the self-consistent potential from a small population in the second subband. From the decrease in transition energy with increasing magnetic field, we can measure not only subband energies but also the values of the effective potential on the acceptor site. The optical intensity oscillations reflect a combination of the small second-subband population and many-electron excitonic effects which enhance the emission intensity at the Fermi level. The many-electron excitonic effects are dominated by the dynamical response of the Fermi sea and would be excluded in the Mahan exciton picture which treats the equilibrium electrons as a rigid Fermi sea.

In the low-density regime, where the second subband plays no role in the equilibrium population, we observe very small oscillations in the energies of the first-subband Landau levels contrary to what is observed for the recombination of electrons with free holes. In our sample, the acceptor is charge neutral in its initial state and so the hole self-energy (which leads to oscillations in the free-hole recombination) is canceled by the screening cloud of the negatively charged acceptor. A weak emission is observed from photoexcited carriers in the second subband, which shows intensity oscillations with a characteristic period $\Delta/\hbar\omega_c$. The oscillations in emission intensity, however, are not accompanied by rapid changes in the line position, in agreement with theory and our picture of a charge neutral acceptor in the initial state. The oscillations of the integrated intensity are thought to be a population effect due to first subband "l" Landau levels crossing the second subband at $l\,\Delta/\hbar\omega_c$.

ACKNOWLEDGMENTS

P.H. wishes to thank Professor K. von Klitzing and Dr. H. Grahn for their hospitality and for partial financial support by the Max-Planck-Institut during his stay in Stuttgart. N.J.P. wishes to thank the Royal Society for financial support.

[1]M. S. Skolnick, K. J. Nash, S. J. Bass, P. E. Simmonds, and M. J. Kane, Solid State Commun. **67**, 637 (1988).

[2]Y. H. Zhang, N. N. Ledentsov, and K. Ploog, Phys. Rev. B **44**, 1399 (1991).

[3]I. V. Kukushkin, K. v. Klitzing, K. Ploog, V. E. Kirpichev, and B. N. Shepel, Phys. Rev. B **40**, 4179 (1990); I. V. Kukushkin, K. von Klitzing, K. Ploog, and V. B. Timofeev, *ibid.* **40**, 7788 (1990); H. Buhmann, W. Joss, K. von Klitzing, I. V. Kukushkin, G. Martinez, A. S. Plaut, K. Ploog, and V. B. Timofeev, Phys. Rev. Lett. **65**, 1056 (1990).

[4]W. Chen, M. Fritze, A. V. Nurmikko, D. Ackley, C. Colvard, and H. Lee, Phys. Rev. Lett. **64**, 2434 (1990); W. Chen, M. Fritze, W. Walecki, A. Nurmikko, D. Ackley, J. M. Hong, and L. L. Chang, Phys. Rev. B **45**, 8464 (1992).

[5]P. E. Simmons, M. S. Skolnick, L. L. Taylor, S. J. Bass, and K. J. Nash, Solid State Commun. **67**, 1151 (1988).

[6]For a general review, see G. D. Mahan, *Many-Particle Physics* (Plenum, New York, 1981); for a review of optical properties of modulation-doped quantum wells, see S. Schmitt-Rink, D. S. Chemla, and D. A. B. Miller, Adv. Phys. **38**, 89 (1989).

[7]A. J. Turberfield, S. R. Haynes, P. A. Wright, P. A. Ford, R. G. Clark, J. F. Ryan, J. J. Harris, and C. T. Foxon, Phys. Rev. Lett. **65**, 635 (1990).

[8]B. B. Goldberg, D. Heiman, A. Pinczuk, L. Pfeiffer, and K. West, Surf. Sci. **263**, 9 (1992); B. B. Goldberg *et al.*, Phys. Rev. Lett. **65**, 641 (1990).

[9]T. Uenoyama and L. J. Sham, Phys. Rev. B **39**, 11 044 (1989).

[10]J. F. Mueller, Phys. Rev. B **42**, 11 189 (1990).

[11]P. Hawrylak, Phys. Rev. B **44**, 6262 (1991); **44**, 3821 (1991).

[12]P. Hawrylak, Phys. Rev. B **44**, 11 236 (1991).

[13]P. Hawrylak, Phys. Rev. B **45**, 4237 (1992).

[14]M. Combescot and P. Nozieres, J. Phys. (Paris) **32**, 913 (1972).

[15]G. D. Mahan, Phys. Rev. B **21**, 1421 (1980).

[16]P. Hawrylak, Phys. Rev. B **42**, 8986 (1990).

[17]T. Rötger, J. C. Maan, P. Wyder, F. Meseguer, and K. Ploog, J. Phys. (Paris) **48**, 389 (1987).

[18]K. Ensslin, D. Heitmann, and K. Ploog, Phys. Rev. B **37**, 10 150 (1988).

[19]D. G. Hayes, M. S. Skolnick, D. M. Whittaker, P. E. Simmonds, L. L. Taylor, S. J. Bass, and L. Eaves, Phys. Rev. B **44**, 3436 (1991).

[20]C. H. Perry *et al.*, in *High Magnetic Fields in Semiconductor Physics,* edited by D. Landwehr (Springer-Verlag, Berlin, 1986), p. 202.